International Journal of Control

ISSN: (Print) (Online) Journal homepage: https://www.tandfonline.com/loi/tcon20

# Kernel-based identification of asymptotically stable continuous-time linear dynamical systems

Matteo Scandella , Mirko Mazzoleni , Simone Formentin & Fabio Previdi

**To cite this article:** Matteo Scandella , Mirko Mazzoleni , Simone Formentin & Fabio Previdi (2021): Kernel-based identification of asymptotically stable continuous-time linear dynamical systems, International Journal of Control, DOI: 10.1080/00207179.2020.1868580

**To link to this article:** https://doi.org/10.1080/00207179.2020.1868580

Accepted author version posted online: 04 Jan 2021.

**Publisher:** Taylor & Francis
**Journal:** International Journal of Control
**DOI:** 10.1080/00207179.2020.1868580



# Kernel-based identification of asymptotically stable continuous-time linear dynamical systems

Matteo Scandella[a] , Mirko Mazzoleni[a], Simone Formentin[b] and Fabio Previdi[a]

[a] Department of Management, Information and Production Engineering, University of Bergamo. Via G. Marconi 5, 24044 Dalmine (BG), Italy;
[b] Department of Electronics, Information and Bioengineering, Politecnico di Milano. Via G. Ponzio 34/5, 20133 Milano, Italy.
Received 11 Jun 2020, Revised 23 Oct 2020, Accepted 19 Dec 2020

**ARTICLE HISTORY**
Compiled December 22, 2020

**Abstract**
In many engineering applications, continuous-time models are preferred to discrete-time ones, in that they provide good physical insight and can be derived also from non-uniformly sampled data. However, for such models, model selection is a hard task if no prior physical knowledge is given. In this paper, we propose a non-parametric approach to infer a continuous-time linear model from data, by automatically selecting a proper structure of the transfer function and guaranteeing to preserve the system stability properties. By means of benchmark simulation examples, the proposed approach is shown to outperform state-of-the-art continuous-time methods, also in the critical case when short sequences of canonical input signals, like impulses or steps, are used for model learning.

**KEYWORDS**
Kernel-based learning; Linear identification; Continuous-time identification

## 1. Introduction

System identification, the science of modeling dynamical systems from data, is a widely explored topic (i.a. Ljung & Glad, 2016; Pintelon & Schoukens, 2012). Given the sampled nature of the measurements, the research community has focused most of its efforts on *discrete-time models*.

Methods for both parametric (i.a. Paduart et al., 2010; Pintelon, Guillaume, Rolain, Schoukens, & Hamme, 1994) and non-parametric models (i.a. Rüdinger & Krenk, 2001; Schoukens, Pintelon, Vandersteen, & Guillaume, 1997; Wellstead, 1981) exist, working both within the time (i.a. Paduart et al., 2010; Rüdinger & Krenk, 2001) or the frequency domain (i.a. Pintelon et al., 1994; Schoukens et al., 1997), and devoted to Linear Time Invariant (LTI) (i.a. Pillonetto & De Nicolao, 2010; Rüdinger & Krenk, 2001), Linear Parameter/Time Varying (LPV/LTV) (i.a. Darwish, Cox, Proimadis, Pillonetto, & Tóth, 2018; Golabi, Meskin, Toth, & Mohammadpour, 2017; Shi, Law, & Xu, 2009) or non-linear (i.a. Formentin, Mazzoleni, Scandella, & Previdi, 2019; Mazzoleni, Formentin, Scandella, & Previdi, 2018; Mazzoleni, Scandella, Formentin,

CONTACT Matteo Scandella. Email: m.scandella@imperial.ac.uk

& Previdi, 2018; Mazzoleni, Scandella, & Previdi, 2019; Pillonetto, Quang, & Chiuso, 2011) systems.

Nonetheless, discrete-time models present several drawbacks (see Garnier, 2015; Garnier & Young, 2012, for more details), e.g., they work only with the sampling frequency of the dataset, they cannot handle non-uniformly sampled data, they cannot easily cope with stiff systems and deriving physical insight is difficult.

Such issues can be tackled by switching to *continuous-time models* (Wang & Gawthrop, 2001). In fact, since such models are not intrinsically defined by a certain sampling frequency, the above problems are automatically solved. In this setting, specific algorithms and optimization schemes have been developed during the years for both regularly (i.a. Garnier, 2015; Garnier & Wang, 2008; Padilla, Garnier, Young, Chen, & Yuz, 2019; Young, 2015) and irregularly sampled datasets (i.a. F. Chen, Agüero, Gilson, Garnier, & Liu, 2017; F. Chen, Garnier, & Gilson, 2015).

Most of the aforementioned methods are parametric and require the prior knowledge of the system complexity. When the system order is not known, complexity measures such as the Young Information Criteria (YIC) (Young, 2011) can be employed.

However, complexity criteria such as YIC select the model shape among a finite set of possible structures. This was one of the main reasons for the introduction of non-parametric kernel methods in system identification, where model complexity is tuned in a continuous way. Non-parametric approaches were originally introduced by Pillonetto and De Nicolao (2010) for continuous-time LTI systems, where Bounded-Input Bounded-Output (BIBO) stability of the identified model is guaranteed by the developed *stable-spline* kernel. Since then, identification approaches that rely on kernels have been successfully devised for other continuous-time problems (T. Chen, 2018b; Lataire, Pintelon, Piga, & Tóth, 2017).

Nonetheless, the approach in Pillonetto and De Nicolao (2010) is difficult to implement for practical use, due to the need of analytically deriving the kernel matrix. In continuous time, this involves the integrals of the input signal $u(t)$ and the kernel function $k(\cdot, \cdot)$. As noticed in Dinuzzo (2015), those integrals can be computed in closed form only if the input signal is known to have a sufficiently simple expression. For this reason, the discrete-time version of kernel methods is mostly used in practice, followed by the identification of a high-order Finite Impulse Response (FIR) model using the obtained non-parametric estimate. If a continuous-time parametric transfer function is needed, then the user has to resort to a two-steps approach: **(i)** perform an order reduction of the high-order FIR model; **(ii)** convert the discrete-time reduced model to a continuous-time one.

In this work, we provide a novel approach for *direct* non-parametric continuous-time identification of the transfer function of asymptotically stable LTI systems. The method is indeed inspired to the work of Pillonetto and De Nicolao (2010), but it directly computes the estimate of the transfer function of the system, thus not needing to compute the impulse response first and then project it onto a suitable system of the Laplace domain. In particular, the proposed approach:

- automatically selects the best transfer function complexity from the available data;
- can be used with practically low-exciting signals like the Dirac impulse or the step[1];

[1]Here, the notion of "low excitation" is not referring to the spectral density of the theoretical impulse and step signals, which have a flat spectrum, but to the spectrum of their finite time realizations, which are known not to share the same excitation properties.

- guarantees the *asymptotic stability* of the identified transfer function. Note that the method of (Pillonetto & De Nicolao, 2010) only ensures the *BIBO stability* of the impulse response. Moreover, this property is not guaranteed to be preserved during the transformation of the impulse response into a transfer function.

The remainder of this paper is as follows. Section 2 briefly reviews the kernel-based approach for continuous LTI system identification of (Pillonetto, Dinuzzo, Chen, De Nicolao, & Ljung, 2014). Furthermore, a novel general parametrization of stable-spline kernel is presented. Section 3 illustrates the estimation method proposed in this paper. Then, the developed approach is compared with the `CONTSID toolbox` (Garnier & Gilson, 2018; Pascu, Garnier, Ljung, & Janot, 2019) in Section 4. The paper ends with some concluding remarks.

## 2. Non-parametric impulse response estimation

In this section:

- we review the basics of kernel methods for LTI system identification;
- we introduce the stable-spline kernel;
- we provide a novel general parametrization of the stable-spline kernel.

### *2.1. Review of kernel methods and problem statement*

Consider the continuous causal Single-Input Single-Output (SISO) LTI system with impulse response $\breve{g} : \mathbb{R} \to \mathbb{R}$. Then, the input/output relation of the system is

$$y(t) = [\breve{g} \star u](t) = \int_0^{+\infty} \breve{g}(\xi)\, u(t-\xi)\, d\xi, \tag{1}$$

where $u : \mathbb{R}_+ \to \mathbb{R}$ and $y : \mathbb{R}_+ \to \mathbb{R}$ are, respectively, the input and the output signals, and $\star$ denotes the convolution operator. In the Laplace domain, this relation becomes

$$Y(s) = \breve{G}(s)\, U(s), \tag{2}$$

where, being $\mathcal{L}$ the Laplace operator, $U(s) = \mathcal{L}[u](s)$, $Y(s) = \mathcal{L}[y](s)$ and $\breve{G}(s) = \mathcal{L}[\breve{g}](s)$ is the transfer function of the system.

Suppose to have at disposal a dataset containing $n \in \mathbb{N} \setminus \{0\}$ noisy measurements, obtained with an experiment on the plant

$$\mathcal{D} = \{(t_i, y_i), 1 \leq i \leq n\}, \tag{3}$$

distributed according to the probabilistic model

$$y_i = [\breve{g} \star u](t_i) + e_i, \qquad i = 1, \ldots, n \tag{4}$$

where $e_i \sim \mathcal{N}(0, \eta^2)$ are independent and identically distributed output-error Gaussian noises and $u : \mathbb{R} \to \mathbb{R}$ is the known input excitation used during the experiment. For the remainder of the manuscript, we will assume that the time instants $t_i$ are in

chronological order, i.e. $t_i \geq t_{i-1}$, $i = 2, \ldots, n$ and the excitation signal $u(t)$ is applied to the plant at the time instant $d \in \mathbb{R}$, i.e. $u(t) = 0$, $\forall t < d$. We will, also, suppose that all the time-instants $t_i$ are strictly greater than $d$ because, thanks to the causality of the system, all others time instants do not contribute to the output computation, and they can be discarded from the dataset.

The aim is now to estimate the (continuous-time) impulse response $\breve{g}$ of the SISO LTI system under analysis using the noisy dataset $\mathcal{D}$ and the knowledge of the shape of the excitation $u(t)$ (in other words, the analytic expression of $u(t)$ is supposed to be exactly known). Following the rationale developed by Pillonetto and De Nicolao (2010), we can estimate $\breve{g}$ by

$$\begin{aligned} \hat{g} &= \arg\min_{g \in \mathcal{H}_k} \left\{ J(g) \right\}, \\ J(g) &= \sum_{i=1}^{n} \left( y_i - [g \star u](t_i) \right)^2 + \tau \|g\|_{\mathcal{H}}^2, \end{aligned} \tag{5}$$

where $\mathcal{H}$ is a Reproducing Kernel Hilbert Space (RKHS) with kernel $k : \mathbb{R}_+ \times \mathbb{R}_+ \to \mathbb{R}$, $\tau > 0$ controls the regularization strength and $\|\cdot\|_{\mathcal{H}}$ is the induced norm of the space $\mathcal{H}$. We suppose that the kernel $k$ depends on some hyper-parameters $\boldsymbol{\rho} \in \mathbb{R}^{n_\rho \times 1}$. The first term of the cost function $J$ in (5) is a loss term that becomes smaller when the model has a good fit on the dataset, while the second one is a regularization term that penalizes more complex models.

As explained by Dinuzzo and Schölkopf (2012), this estimator can be written as

$$\hat{g}^u(t) = \sum_{i=1}^{n} c_i \hat{g}_i^u(t), \tag{6}$$

where the dependency on the input shape $u(t)$ is highlighted and

$$\hat{g}_i^u(t) = \int_0^\infty u(t_i - \xi)\, k(t, \xi)\, d\xi. \tag{7}$$

The coefficients vector $\boldsymbol{c} = [c_1, \ldots, c_n]^\top \in \mathbb{R}^{n \times 1}$ can be found by solving the linear system

$$\boldsymbol{O}(\boldsymbol{O} + \tau \boldsymbol{I}_n)\, \boldsymbol{c} = \boldsymbol{O}\boldsymbol{y}^\top, \tag{8}$$

where $\boldsymbol{y} = [y_1, \ldots, y_n] \in \mathbb{R}^{1 \times n}$ and $\boldsymbol{O} \in \mathbb{R}^{n \times n}$ is a symmetric positive-semidefinite matrix whose $(i, j)$ element is $o^u(t_i, t_j)$, given by

$$o^u(t_i, t_j) = \int_0^{+\infty} \int_0^{+\infty} u(t_i - \psi)\, u(t_j - \xi)\, k(\psi, \xi)\, d\xi\, d\psi. \tag{9}$$

The computation of (7) and (9) is the main obstacle that makes difficult to implement kernel methods in continuous time. We again remark here that the integrals in (7) and (9) can be computed analytically for certain classes of kernels and inputs signals; otherwise, they can be approximated numerically, see Dinuzzo (2015). In this

work, we derive a closed-form solution for two widely used input signals in the control community, i.e. impulse and step inputs, by relying on the so-called stable-spline kernel.

The tuning of the hyper-parameters of the method $\boldsymbol{\zeta} = \left[\boldsymbol{\rho}^\top, \tau\right]^\top \in \mathbb{R}^{n_\zeta \times 1}$ can be performed by resorting to its Bayesian interpretation (Pillonetto et al., 2014).

The model described in (4) gives the likelihood distribution $p\left(\boldsymbol{y}|g, \boldsymbol{\zeta}\right)$, where $g$ is a generic impulse response function. Imposing a Gaussian stochastic process prior $p\left(g|\boldsymbol{\zeta}\right)$ on the impulse response allows obtaining a posterior $p\left(g|\boldsymbol{y}, \boldsymbol{\zeta}\right)$, whose expected value is equal to the estimator (6). From this different point of view, it is possible to compute the marginal likelihood density function as

$$p\left(\boldsymbol{y}|\boldsymbol{\zeta}\right) = \int p\left(\boldsymbol{y}|g, \boldsymbol{\zeta}\right) p\left(g|\boldsymbol{\zeta}\right)\, dg = \mathcal{N}\left(\boldsymbol{y}^\top \middle| \mathbf{0}_{n\times 1}, \boldsymbol{O} + \tau \boldsymbol{I}_n\right). \tag{10}$$

This distribution represents the likelihood to have a certain set of measurements $\boldsymbol{y}$ given a certain value of the hyper-parameters $\boldsymbol{\zeta}$. For this reason, it is possible to select the vector $\boldsymbol{\zeta}$ by searching the one that maximizes the likelihood to obtain the set of measurements at our disposal. Therefore:

$$\hat{\boldsymbol{\zeta}} = \underset{\boldsymbol{\zeta} \in \mathbb{R}^{n_\zeta}}{\arg\min} \left\{ \boldsymbol{y} \left(\boldsymbol{O} + \tau \boldsymbol{I}_n\right)^{-1} \boldsymbol{y}^\top + \log\det\left(\boldsymbol{O} + \tau \boldsymbol{I}_n\right) \right\} \tag{11}$$

where, instead of the direct maximization of $p\left(\boldsymbol{y}|\boldsymbol{\zeta}\right)$, the negative log version of $p\left(\boldsymbol{y}|\boldsymbol{\zeta}\right)$ is minimized for convenience and computational reasons.

### *2.2. Stable-spline kernel*

The performance of the estimator $\hat{g}^u$ heavily depends on the employed kernel. In particular, most of them are not suitable for this application since they define RKHS containing functions that correspond to unstable systems. To solve this problem, the so-called *stable kernels* can be used (Pillonetto et al., 2014). An example of this kind of kernel is the stable-spline one $k_q : \mathbb{R}_+ \times \mathbb{R}_+ \to \mathbb{R}$ that is defined as:

$$k_q\left(a, b\right) = \lambda s_q\left(e^{-\beta a}, e^{-\beta b}\right), \tag{12}$$

where $q \in \mathbb{N} \setminus \{0\}$ is the stable-spline order, $\beta$ and $\lambda$ are two strictly positive scalar hyper-parameters and $s_q : [0,1] \times [0,1] \to \mathbb{R}$ is the regular spline kernel of order $q$ (Wahba, 1990), i.e.

$$s_q\left(a, b\right) = \int_0^1 G_q\left(a, x\right) G_q\left(b, x\right)\, dx, \tag{13}$$

where

$$G_q\left(a, x\right) = \frac{1}{(q-1)!} \begin{cases} (a-x)^{q-1} & \text{if } a \geq x \\ 0 & \text{if } a < x \end{cases}. \tag{14}$$

Notice that the $\lambda$ hyper-parameter is related to the static gain of the system at hand, while $\beta$ defines its bandwidth. In the literature it is possible to find other stable kernels like the continuous DC kernel (T. Chen, Ohlsson, & Ljung, 2012). T. Chen (2018b) presented a detailed analysis on how to select the right stable-kernel for system identification.

In this manuscript, the focus will be on the stable-spline kernel (Pillonetto et al., 2014) because they are widely studied and used in a wide range of applications. For example, in addition to their use in LTI system identification, the stable-spline kernel can be employed for hybrid systems' identification (Pillonetto, 2015), for blind systems' identification (Bottegal, Risuleo, & Hjalmarsson, 2015), for Hammerstein systems' identification (Risuleo, Bottegal, & Hjalmarsson, 2015), for identification with missing data (Pillonetto, Chiuso, & De Nicolao, 2019), for robust identification Pillonetto, Carè, and Campi (2018) and with other type of regularizations (Aravkin, Burke, & Pillonetto, 2018). Furthermore, the stable splines have been extensively studied and their behavior is well documented (T. Chen et al., 2016; Pillonetto, 2018). It has also been shown that the DC kernel and the TC kernel, two other widely used kernels in these settings, are strongly related to the stable splines (T. Chen, 2018a).

In particular, a generic order stable-spline kernel can be represented as follows.

**Proposition 1** (Spline kernels)**.** *The spline kernel $s_q : [0,1] \times [0,1] \to \mathbb{R}$ of order $q$ and the stable-spline kernel $k_q : \mathbb{R}_+ \times \mathbb{R}_+ \to \mathbb{R}$ of order $q$ can be written, respectively, as:*

$$s_q(a,b) = \sum_{h=0}^{q-1} \gamma_{q,h} \begin{cases} a^{2q-h-1} b^h & \text{if } a \leq b \\ b^{2q-h-1} a^h & \text{if } a > b \end{cases}, \tag{15}$$

$$k_q(a,b) = \lambda \cdot \sum_{h=0}^{q-1} \gamma_{q,h} \begin{cases} e^{-\beta[(2q-h-1)a+hb]} & \text{if } a \geq b \\ e^{-\beta[(2q-h-1)b+ha]} & \text{if } a < b \end{cases}, \tag{16}$$

*where*

$$\gamma_{q,h} = \frac{(-1)^{q+h-1}}{h!\,(2q-h-1)!} \tag{17}$$

***Proof.*** The proof is reported in the appendix on page 17. ■

**Remark 1.** From Proposition 1, we can see that the stable-spline kernel of order $q$ is a weighted sum of $q$ negative exponential terms. For this reason, the stable-spline kernel is easily computable for every order $q$. This novel formulation allows treating $q$ as an additional hyper-parameter, i.e. $\boldsymbol{\zeta} = [\lambda, \beta, q, \tau]$. Thus, it is possible to obtain a better data-fit with respect to fixing the spline order value in advance. In this case, the optimization of (11) becomes a mixed real-integer optimization problem that requires suitable techniques. However, a greedy (sub-optimal) solution for this problem is to select the order $q$ with an exhaustive search from a certain pool of values.

The estimator $\hat{g}^u$, as defined in (6), gives a continuous-time non-parametric representation of the system, in terms of its impulse response. For practical applications, however, like control design and behavior analysis, this representation is not as useful as the transfer function one. To achieve this, the current practice consists of two steps procedure (T. Chen et al., 2012; Mazzoleni, Scandella, et al., 2018):

1. perform a discrete-time non-parametric estimate of the system impulse response by fitting a high-order FIR model on the available dataset;
2. convert the discrete-time transfer function to a continuous-time one.

The next section presents the proposed method, where a direct procedure is proposed to estimate the continuous-time system transfer function.

## 3. Asymptotically stable transfer function estimation

This section presents the proposed approach for continuous-time system identification. Specifically, we:

- explain the main rationale of the method;
- show the method using impulse inputs;
- exemplify the method using step inputs.

### *3.1. Continuous-time transfer function identification*

To start with, consider the following proposition that relates estimated impulse response with the transfer function of the system:

**Proposition 2** (TF expression)**.** *Given the non-parametric estimator $\hat{g}^u$, as explained in* (6)*, of an LTI system, the corresponding transfer function is*

$$\hat{G}^u(s) = \sum_{i=1}^{n} c_i \hat{G}_i^u(s), \tag{18}$$

*where*

$$\hat{G}_i^u(s) = \int_d^{t_i} u(\tau) K(s; t_i - \tau)\, d\tau, \tag{19}$$

*and*

$$K(s; x) = \int_0^{\infty} k(t, x)\, e^{-st}\, dt. \tag{20}$$

***Proof.*** The proof is reported in the appendix on page 22. ■

From the above result, it is possible to note that the estimated transfer function is composed of the convolution of two terms: the first one, $u(x)$, depends only on the shape of the excitation signal while the second one, $K(s; t_i - x)$, depends only on the kernel used.

For the stable-spline kernel of generic order $q$, it is possible to compute a more informative formulation thanks to the following proposition.

**Proposition 3** (Stable spline TF expression)**.** *Let the kernel be a stable-spline $k_q$ of order $q$ and $u_i(t) = u(t_i - t)$. The identified transfer function can be written as*

$$\hat{G}^u(s) = \lambda \left[ \sum_{h=0}^{q-1} Q_{q,h}^u(s) + H_q^u(s) \right], \tag{21}$$

*where*

$$Q_{q,h}^u(s) = \frac{\gamma_{q,h}}{s + \beta h} \cdot \left( \sum_{i=1}^{n} c_i \cdot A_i^u(\beta(2q - h - 1)) \right) \tag{22}$$

$$H_q^u(s) = \frac{(-1)^q \beta^{2q-1}}{\prod_{i=0}^{2q-1}(s + \beta i)} \cdot \left( \sum_{i=1}^{n} c_i \cdot A_i^u(s + \beta(2q - 1)) \right) \tag{23}$$

*and*

$$A_i^u(x) = \mathcal{L}[u_i](x). \tag{24}$$

***Proof.*** The proof is reported in the appendix on page 23. ■

The expression (21) represents the estimated transfer function as a sum of $q + 1$ transfer functions. The first $q$ of them have one real pole located in a multiple of $-\beta$ and a gain that depends on the coefficients $\boldsymbol{c}$, the hyper-parameters $\lambda$ and $\beta$, the spline order and the shape of the input signal $u(t)$. The last one has $2q - 1$ real poles that are multiple of $-\beta$ and, eventually, other poles that depend on the shape of the input $u(t)$. In particular, the term $A_i^u(s + \beta(2q - 1))$ can have some poles or zeros that will be added to $\hat{G}^u$.

The following theorem relates choice of the input signal $u(t)$ with the asymptotic stability of the identified model.

**Theorem 1** (Excitation for stability)**.** *If the experiment excitation $u(x)$, used to collect the dataset $\mathcal{D}$, is such that the terms*

$$A_i^u(s + \beta(2q - 1)), \qquad i = 1, \ldots, n \tag{25}$$

*are functions whose poles have a negative real part, then the identified transfer function $\hat{G}^u(s)$ is asymptotically stable.*

***Proof.*** The proof is reported in the appendix on page 26. ■

From this Theorem, it is clear that the terms (25) have an important role in the identification procedure and on the stability of the identified model. Furthermore, note that the identified model is always at least BIBO stable because the stable-spline kernel is a stable kernel.

The proposed identification method is described in Algorithm 1. In particular, the following quantities, that depend on the excitation signal used for the experiment and on the employed kernel, have to be defined:

- the derived kernel $o^u$ as described in (9);
- the identified transfer function $\hat{G}_u$ as described in Proposition 2. If the kernel used is a stable-spline, then the Proposition 3 can be employed.

**Algorithm 1:** Asymptotically stable transfer function estimation

**Input:** The dataset $\mathcal{D}$
**Input:** A way to compute $o^u$ given $\boldsymbol{\zeta} = [\lambda, \beta, \tau, q]$ and two time instants
**Input:** A way to compute $\hat{G}^u$ given $\boldsymbol{\zeta} = [\lambda, \beta, \tau, q]$ and $\boldsymbol{c}$

1 Discard the part of the dataset $\mathcal{D}$ corresponding to time instants $t_i \leq d$
2 Find the optimal hyper-parameters $\widetilde{\boldsymbol{\zeta}}$ by minimizing equation (11)
3 Compute the matrix $\boldsymbol{O}$ using the hyper-parameters $\widetilde{\boldsymbol{\zeta}}$
4 Compute a valid solution $\boldsymbol{c}$ of the linear system (8)
5 Compute $\hat{G}^u$ given $\widetilde{\boldsymbol{\zeta}}$ and $\boldsymbol{c}$

**Output:** The transfer function $\hat{G}^u$

In next sections, Algorithm 1 is applied to the impulse and step input signals. These two signals are widely used in practical applications due to the simplicity of the experimental setup needed for their use on the plant. Furthermore, some of the most common system identification techniques, such as PEM (Ljung & Glad, 2016) or FRF identification (Pintelon & Schoukens, 2012), require more complex input signals to work effectively (e.g. white noise or multisine signals).

It is also important to note that the same methodology can be extended to more complex input signals such as polynomials, sinusoidals or combinations of all the above. This extension is left to future research.

**Remark 2.** The computational complexity of the proposed method does not differ significantly with respect to the traditional kernel methods, because the most time-consuming task is the computation of the coefficients $\boldsymbol{c}$. The computation of this task is widely studied in the literature in both computational and memory complexities (Rudi, Camoriano, & Rosasco, 2015; Rudi, Carratino, & Rosasco, 2017; Scandella, Mazzoleni, Formentin, & Previdi, 2020).

### *3.2. Identification using impulse response data*

Consider the case where the input signal is a Dirac impulse, applied at the time instant $d \in \mathbb{R}$, i.e.

$$u(t) = \mathrm{imp}(t) = \delta(t - d). \tag{26}$$

In this case we have

$$\mathrm{imp}_i(t) = \mathrm{imp}(t_i - t) = \delta(t_i - t - d) = \delta(t - (t_i - d)). \tag{27}$$

Therefore, since $t_i > d$, we have

$$A_i^{\mathrm{imp}}(x) = \mathcal{L}[\mathrm{imp}_i](x) = e^{-x(t_i - d)} \tag{28}$$

Thus, it is straightforward to check the condition of Theorem 1. In particular, we have:

$$A_i^{\mathrm{imp}}(s + \beta(2q-1)) = e^{-(s+\beta(2q-1))(t_i-d)} = e^{-\beta(2q-1)(t_i-d)} \cdot e^{-s(t_i-d)}. \tag{29}$$

This is an input-output delay with a certain gain. Therefore, it is asymptotically stable and the required condition is respected for every value of the hyper-parameters and for every time instant $t_i > d$. Furthermore, applying Theorem 2 and using (28), we can compute the identified transfer function $\hat{G}^{\text{imp}}$, as

$$\hat{G}^{\text{imp}}(s) = \lambda \left[ \sum_{h=0}^{q-1} Q_{q,h}^{\text{imp}}(s) + H_q^{\text{imp}}(s) \right] \tag{30}$$

$$Q_{q,h}^{\text{imp}}(s) = \frac{\gamma_{q,j}}{s+\beta h} \sum_{i=1}^{n} c_i e^{-\beta(2q-h-1)(t_i-d)} \tag{31}$$

$$H_q^{\text{imp}}(s) = \frac{(-1)^q \beta^{2q-1}}{\prod_{i=0}^{2q-1}(\beta i + s)} \sum_{i=1}^{n} c_i e^{-\beta(2q-1)(t_i-d)} \cdot e^{-s(t_i-d)} \tag{32}$$

The transfer function $H_q^{\text{imp}}(s)$ is *not rational*. In particular, the numerator is composed by a sum of weighted input-output delays. To highlight this fact, we can define

$$T_q^{\text{imp}}(s) = \sum_{i=1}^{n} c_i e^{-\beta(2q-1)(t_i-d)} \cdot e^{-s(t_i-d)} \tag{33}$$

in order to isolate the non-rational part of $H_q^{\text{imp}}(s)$, i.e.

$$H_q^{\text{imp}}(s) = \frac{(-1)^q \beta^{2q-1}}{\prod_{i=0}^{2q-1}(\beta i + s)} T_q^{\text{imp}}(s). \tag{34}$$

**Remark 3.** Non-rational transfer functions are difficult to manage and, in general, classical dimensionality reduction algorithms, such as the balance reduction (Varga, 1991), does not work on this type of models. For these reasons, it is useful to develop a way to find a rational approximation $\widetilde{T}_q^{\text{imp}}(s)$ of $T_q^{\text{imp}}(s)$. This is hereby achieved using a Padé approximant (Baker & Graves-Morris, 1996). In particular, a specialized approximant for $T_q^{\text{imp}}(s)$ of order 25 was developed following the rationale described by Baker and Graves-Morris (1996).

In order to implement the proposed identification procedure, it is also necessary to compute the derived kernel (9) in the specific case at hand. For this case (i.e. impulse input signal and stable-spline kernel), we have

$$o_q^{\text{imp}}(t_i, t_j) = \lambda \sum_{h=0}^{q-1} \gamma_{q,h} \begin{cases} e^{-\beta[(2q-h-1)a+hb]} & \text{if } a \geq b \\ e^{-\beta[(2q-h-1)b+ha]} & \text{if } a < b \end{cases}. \tag{35}$$

### *3.3. Identification using step response data*

Consider now the case where a step input is applied at the time instant $d \in \mathbb{R}$, i.e.

$$u(t) = \text{step}(t) = \begin{cases} 1 & \text{if } t \geq d \\ 0 & \text{if } t < d \end{cases}. \tag{36}$$

In this case we have

$$\text{step}_i(t) = \text{step}(t_i - t) = \begin{cases} 1 & t \leq t_i - d \\ 0 & t > t_i - d \end{cases} \tag{37}$$

Therefore, since $t_i > d$, we have

$$A_i^{\text{step}}(x) = \mathcal{L}[\text{step}_i](x) = \frac{1}{x} - \frac{e^{-x(t_i-d)}}{x} = \frac{1 - e^{-x(t_i-d)}}{x} \tag{38}$$

Therefore, it is possible to check the condition of Theorem 1. In particular, we have:

$$A_i^{\text{step}}(s + \beta(2q-1)) = \frac{1 - e^{-(s+\beta(2q-1))(t_i-d)}}{s + \beta(2q-1)} \tag{39}$$

$$= \frac{1}{s + \beta(2q-1)} - e^{-s(t_i-d)} \cdot \frac{e^{-\beta(2q-1)(t_i-d)}}{s + \beta(2q-1)}. \tag{40}$$

This is a sum of two transfer functions (the second one with an input-output delay) that share the same pole in

$$p = -\beta(2q-1). \tag{41}$$

Since $q \in \mathbb{N}$, $q \geq 1$ and $\beta > 0$, this pole is strictly negative for every value of the hyper-parameters and the theorem hypothesis is respected.

Applying Theorem 3 and using (38), we can to compute the identified transfer function $\hat{G}^{\text{step}}$

$$\hat{G}^{\text{step}}(s) = \lambda \left[ \sum_{h=0}^{q-1} Q_{q,h}^{\text{step}}(s) + H_q^{\text{step}}(s) \right] \tag{42}$$

$$Q_{q,h}^{\text{step}}(s) = \frac{\gamma_{q,h} \sum_{i=1}^{n} c_i \left(1 - e^{-\beta(2q-h-1)(t_i-d)}\right)}{\beta(2q-h-1)(s+\beta h)} \tag{43}$$

$$H_{q,h}^{\text{step}}(s) = \frac{(-1)^q \beta^{2q-1}}{(s + \beta \cdot (2q-1)) \prod_{i=0}^{2q-1} (\beta i + s)} \cdot \left( \sum_{i=1}^{n} c_i - T_q^{\text{step}}(s) \right) \tag{44}$$

$$T_q^{\text{step}}(s) = \sum_{i=1}^{n} c_i e^{-\beta(2q-1)(t_i-d)} \cdot e^{-s(t_i-d)} \tag{45}$$

Again, we can note that the transfer function $H_q^{\text{step}}(s)$ contains a non-rational term $T_q^{\text{step}}(s)$ that also appears in the identified transfer function obtained using a Dirac impulse as excitation signal. Following the same rationale used in Section 3.2, this non-rational term is approximated using a specialized Padé approximant as explained in Remark 3. The derived kernel (9) in this specific case (i.e. step input signal and stable-spline kernel) reads as

$$o^{\text{step}}(t_i, t_j) = \sum_{h=0}^{q-1} \gamma_{q,h} \begin{cases} w_h(t_i - d, t_j - d) & \text{if } t_i \geq t_j \\ w_h(t_j - d, t_i - d) & \text{if } t_i < t_j, \end{cases} \tag{46}$$

where the term $w_h(a,b)$, when $h=0$, is equal to

$$w_0(a,b) = 2 \cdot \frac{1 - e^{-\beta b(2q-1)}}{\beta^2 (2q-1)^2} - b \cdot \frac{e^{-\beta a(2q-1)} + e^{-\beta b(2q-1)}}{\beta (2q-1)}; \tag{47}$$

instead, for $h > 0$, $w_h(a,b)$ is equal to:

$$w_h(a,b) = 2 \cdot \frac{1 - e^{-\beta b(2q-1)}}{\beta^2 (2q-h-1)(2q-1)} + \\ - \frac{e^{-\beta a(2q-h-1)} \left(1 - e^{-\beta hb}\right)}{\beta^2 h (2q-h-1)} + \frac{e^{-\beta b(2q-1)} \left(1 - e^{\beta hb}\right)}{\beta^2 h (2q-h-1)}. \tag{48}$$

## 4. Simulation examples

In the last decades, continuous-time system identification was studied in detail by Garnier (2015); Garnier and Wang (2008). The most recent methods are implemented in the `CONTSID toolbox` (Garnier & Gilson, 2018; Pascu et al., 2019). This section shows simulation results, where we:

- formulate the simulation setup;
- perform identification on benchmark systems using impulse and step inputs, using the proposed method;
- compare the Simple Refined Instrumental Variable (SRIVC) method (Garnier, 2015; Young, 2011) from the literature with the proposed approach;
- compare the proposed method with the current two-step procedure that first identifies a discrete-time model and then converts it to a continuous-time one, described at the end of Section 2;
- evaluate the sensitivity of the proposed method to a model order reduction procedure.

### *4.1. Simulation setup*

The proposed method is tested on three different asymptotically stable LTI systems:

$$G_1(s) = \frac{27}{20} \cdot \frac{-2000s^3 - 3600s^2 - 2095s - 396}{1350s^4 + 7695s^3 + 12852s^2 + 7796s + 1520} \tag{49}$$

$$G_2(s) = 1600 \cdot \frac{-4s + 1}{s^4 + 5s^3 + 408s^2 + 416s + 1600} \tag{50}$$

$$G_3(s) = \frac{1}{2} \cdot \frac{-30254s^3 - 156761s^2 - 328016s - 888265}{5000s^4 + 82598s^3 + 327672s^2 + 1175044s + 1464739} \tag{51}$$

Figure 1 depicts the magnitude Bode diagrams of the benchmark examples.

The first model $G_1(s)$ behaves like a low-pass filter with a negative gain and it generates a smooth impulse and step responses. Vice-versa the third model $G_3(s)$ produces an oscillating responses. Therefore, these two models are chosen to represent these two opposite scenarios. Lastly, the second model $G_2(s)$ is the Rao-Garnier

benchmark, developed by Garnier (2015); Rao and Garnier (2002), a very common benchmark for continuous system identification.

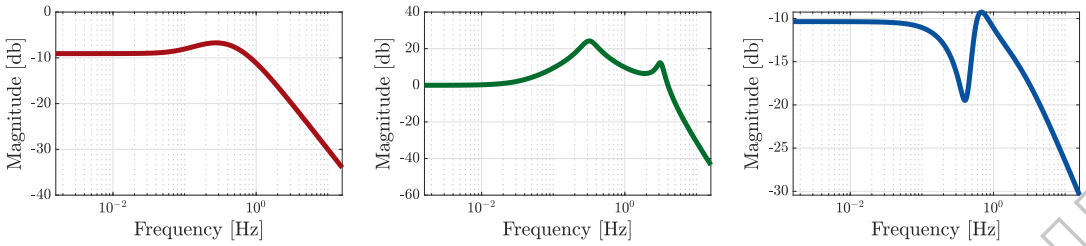


**Figure 1.** Bode diagrams of the three example systems. From left to right: $G_1(s)$, $G_2(s)$ and $G_3(s)$.

In the next parts of this section, the following methodologies are compared:

**A.** The `SRIVC` algorithm, as implemented in the `CONTSID toolbox`, with the knowledge of true number of poles and zeros of systems.

**B.** The `SRIVC` algorithm where the number of zeros and poles is selected between 1 and 5 using the YIC (Young Information Criterion, see Young, 2011, for more details).

**C.** The two steps procedure that first identifies a discrete-time model and then converts it to a continuous-time one. In particular, the identification step is performed using the function `impulseest` of the Matlab System identification Toolbox, using a cubic stable-spline for the regularization. The conversion step is performed using the `d2c` function of the Matlab Control System toolbox, using the Tustin method.

**D.** The proposed algorithm, with a regularly sampled dataset and the stable-spline kernel, with order $q$ chosen in the set $\{1, 2, 3\}$.

**E.** The proposed algorithm, with an irregularly sampled dataset and the stable-spline kernel, with order $q$ chosen in the set $\{1, 2, 3\}$. The time instant are sampled uniformly.

**F.** The proposed algorithm, with an irregularly sampled dataset and the stable-spline kernel, with order $q$ chosen in the set $\{1, 2, 3\}$. The time instant are sampled from a distribution skewed towards the beginning of the experiment.

The output of the true model is compared with the estimated one on a test dataset, obtained using a random white Gaussian noise with 5 Hz of bandwidth as excitation signal. Both input and output are sampled for 1000 s with a sampling frequency of 200 Hz. Then, the performance is computed according to the following fit index

$$\text{Fit} = \left(1 - \frac{\sum_{t=1}^{n_v} (y_t - \hat{y}_t)^2}{\sum_{t=1}^{n_v} \left(y_t - \sum_{t=1}^{n_v} y_t\right)^2}\right) \cdot 100\%, \tag{52}$$

where $n_v$ is the length of the obtained dataset, $y_t$ and $\hat{y}_t$, with $t = 1, \ldots, n_v$, are, respectively, the samples of the true and estimated responses.

### *4.2. Identification performance*

To evaluate the performance of the five methods previously explained, a Monte Carlo simulation was performed with $m = 200$ runs. In particular, given the input $u =$

| System | $T$ | $\eta^2_{imp}$ | $\eta^2_{step}$ |
|---|---|---|---|
| $G_1(s)$ | $4\,s$ | $6.97 \cdot 10^{-2}$ | $7.46 \cdot 10^{-2}$ |
| $G_2(s)$ | $12\,s$ | $7.37 \cdot 10^{-1}$ | $3.69 \cdot 10^{-1}$ |
| $G_3(s)$ | $3\,s$ | $7.56 \cdot 10^{-2}$ | $5.30 \cdot 10^{-2}$ |

**Table 1.** Parameters of the simulation tests for the benchmark models.

$\{\text{imp}, \text{step}\}$, the $m$ different datasets are sampled as

$$e_i \sim \mathcal{N}\left(0, \eta_u^2\right), \qquad i = 1, \ldots, n \tag{53}$$
$$y_i = r_u\left(t_i\right) + e_i, \qquad i = 1, \ldots, n \tag{54}$$

where $n = 250$, $\eta_{\text{imp}}$ and $\eta_{\text{step}}$ for each system as reported in Table 1 and $r_u$ is the response of the system to the input $u$. The noise variances $\eta_{\text{imp}}$ and $\eta_{\text{step}}$ are selected to have Signal-to-Noise-Ratio (SNR) of about 5. The time-instants $t_i$ are sampled in three different ways:

- For the methods **A.**, **B.**, **C.** and **D.**, they are sampled regularly

$$t_i = \frac{T \cdot i}{n}; \tag{55}$$

- For the method **E.**, they are sampled uniformly

$$t_i \sim \mathcal{U}\left(0, T\right); \tag{56}$$

- For the method **F.**, they are sampled from the following distribution

$$b_i \sim \mathcal{B}\left(1, 3.5\right) \tag{57}$$
$$t_i = T \cdot b_i \tag{58}$$

where $T$ changes for each system as reported in Table 1.

Note that the methods **A.**, **B.** and **C.** cannot be applied using an impulse excitation (due to the difficulty of practically obtaining a sampled version of this input[2]) and irregularly sampled data.

The fit index (52) is then computed for the $m$ different datasets for each system and for both impulse and step inputs. Results are shown in Figure 2 for $u = \text{imp}$ and in Figure 3 for $u = \text{step}$, using the classical boxplot notation explained in details in (Velleman & Hoaglin, 1981, Chapter 3).

From these plots, it is clear that the proposed method outperforms the most commonly used procedure for continuous-time system identification in these settings. It is important to note that the methods **A.**, **B.** and **C.** require a persistently exciting input signal instead of a low-exciting one, like those used in these experiments. It can also be noted that the `SRIVC` algorithm has worse performance when the true system order is known (method **A.**) with respect to the case where the order is estimated

[2] In the case of experiments with impulsive input, one solution to perform system identification is to leverage output data by using subspace methods.

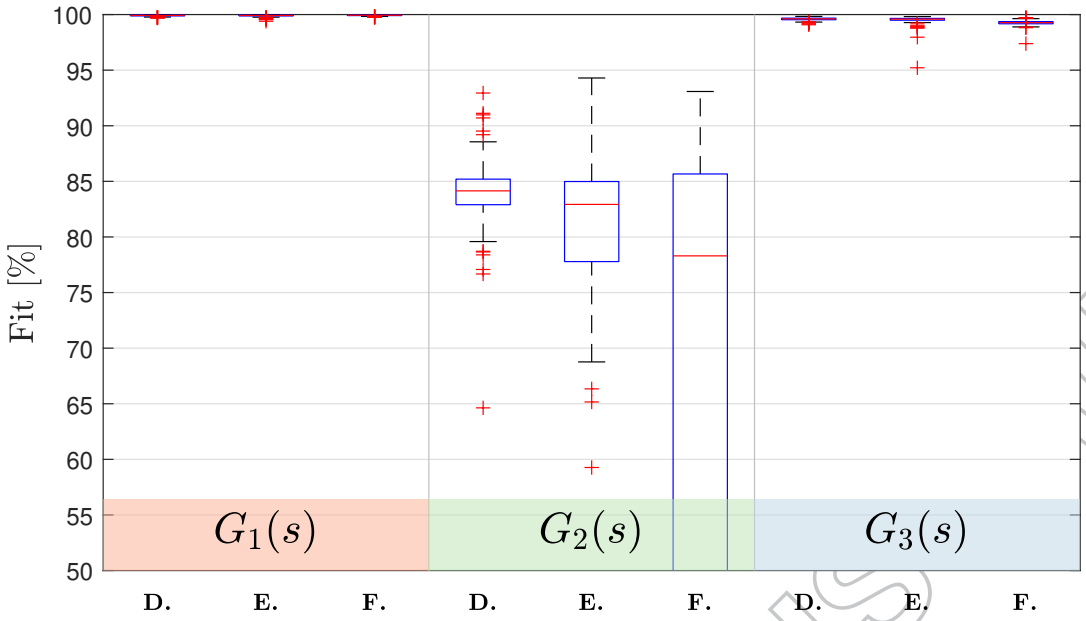


**Figure 2.** Performance of the considered methodologies on the three selected systems using impulse response data.

from the dataset (method **B.**). This is due to the fact that some modes of the system are completely hidden in the measured output data, due to the high noise level, see Figure 4. However, the proposed method (method **D.**) overcomes the limitations of the other methods thanks to a flexible way to select the model order and the specialization on the low-exciting input signals employed.

Furthermore, using a uniformly sampled dataset (method **E.**) the performance does not change significantly with respect to method **D.**. Instead, using a skewed distribution (method **F.**), the performance varies. In particular, using a step excitation they tend to increase and with an impulse input they decrease. The reason behind the latter fact needs further investigation, and we leave it for future work.

To further verify these conclusions, the same experiment was repeated on 200 randomly generated asymptotically stable systems of order 6. In particular, the datasets are generated as reported in (53) and (54) where $n = 500$, $T$ is equal to the settling time of the system and $\eta_u^2$ is selected in such a way that the SNR is 10. Then, the performance are computed with the fit index described in (52), on a test dataset generated in the same way as described before. The obtained results for both impulse and step input are shown in Figure 5.

### *4.3. Sensitivity to dimensional reduction*

Depending on the estimated stable-spline order $q$, the identified transfer function could turn out to be too complex. This section evaluates how dimensionality reduction procedures affect the final model estimate. Here, we employ the Balance Reduction algorithm proposed by Varga (1991).

Consider the case of identification of the benchmark system $G_2(s)$ using impulse response data, as described in Section 4.2. Here, the Monte Carlo simulation returned $m = 200$ identified models. Let $n^i$ be the order of the $i$-th identified model and $\sigma_1^i \geq \ldots \geq \sigma_{n^i}^i$ be the singular values of its Hankel matrix. Then, the model can be

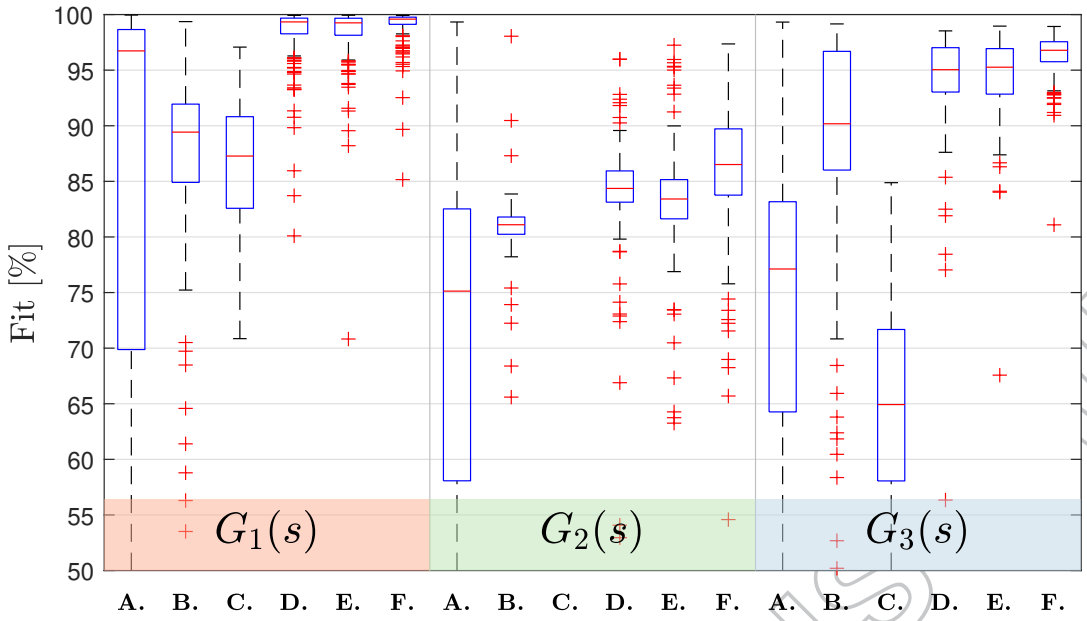


**Figure 3.** Performance of the considered methodologies on the three selected systems using step response data.

reduced to the order

$$w^i = \max\left\{1, \ldots, p^i\right\}$$
$$\text{s.t.} \sum_{j=1}^{w^i} \sigma_j^i \leq \lambda \cdot \sum_{j=1}^{p^i} \sigma_j^i \tag{59}$$

where $\lambda \in [0, 1]$ is the desired level of reduction. It is straightforward to see that smaller values of $\lambda$ lead to smaller orders $w^i$ and vice-versa.

Figure 7 depicts the bar diagram of the non-reduced orders $p^i$ (in the first row) of the identified models and the reduced order $w^i$ at different level of reduction $\lambda$ (the true system $G_2(s)$ has order 4). Here, it is possible to note that, even if the proposed method tends to generate complex dynamics, such models are characterized by very redundant dynamical modes. Therefore, their order can be significantly reduced without neglecting important dynamics. This behavior is also confirmed in Figure 6, where it is possible to see the performance of the reduced model on the test dataset as compared to the non-reduced models.

## 5. Concluding remarks

This paper introduced a novel black-box non-parametric continuous-time LTI identification technique that employs the RKHS properties. The proposed methodology directly identifies a transfer function model, can work with irregularly sampled datapoints and guarantees the asymptotically stability of the identified system. The method showed good performance when employed with low-exciting input signals, such as the impulse or the step (vastly used in practice) as compared to the approach proposed of (Garnier, 2015; Garnier & Gilson, 2018). Furthermore, a general parametrization of

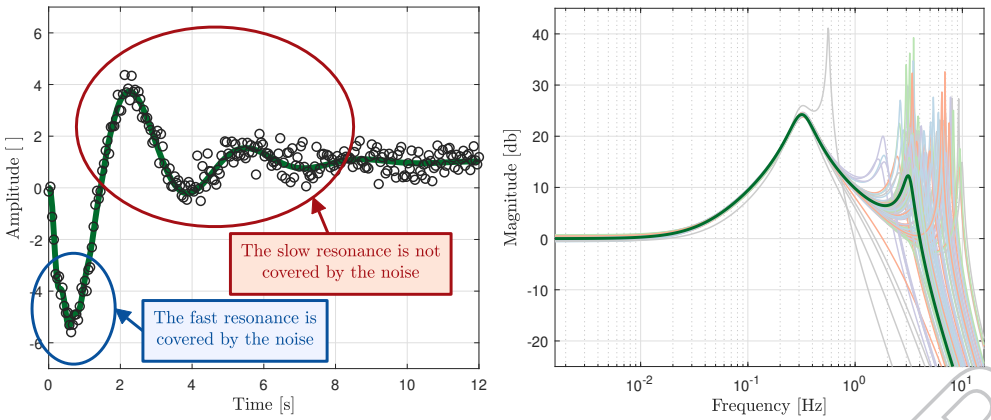


**Figure 4.** Behavior of the `SRIVC` method with known model order (method **A.**) when the noise in the measurements hides a high-frequency low-amplitude resonance. (Left) Time-domain true response and noisy data. (Right) true magnitude Bode diagram and estimated ones on different noise realizations.

the stable-spline kernel is derived, that permits to treat the spline order as an additional tunable hyper-parameter. Future research will be devoted to the development of the proposed method with more general excitation signals and to the experimental validation of the approach on a real-world case study.

## Appendix A. Proofs

***Proof of Proposition 1.*** Firstly, we can note that the term $G_q(a,x)\,G_q(b,x)$ is equal to zero when $a < x \vee b < x$, therefore

$$G_q(a,x)\,G_q(b,x) = \frac{(a-x)^{q-1}(b-x)^{q-1}}{((q-1)!)^2}\begin{cases}1 & \text{if } x \le \min(a,b)\\ 0 & \text{if } x > \min(a,b)\end{cases}$$

following this fact, the integral (13) can be truncated to $\min(a,b)$:

$$s_q(a,b) = \int_0^{\min(a,b)} \frac{(a-x)^{q-1}(b-x)^{q-1}}{((q-1)!)^2}\,dx$$

Let us, now, focus on the case where the first argument of the kernel is greater or equal to the second, i.e. $a \le b$ and $\min(a,b) = a$. Here, thanks to the change of variable $y = a - x$, it is possible to write

$$\begin{aligned} s_q(a,b) &= \frac{1}{((q-1)!)^2}\int_a^0 -y^{q-1}\left(b-(a-y)\right)^{q-1}\,dy \\ &= \frac{1}{((q-1)!)^2}\int_0^a \left((b-a)\,y+y^2\right)^{q-1}\,dy. \end{aligned}$$

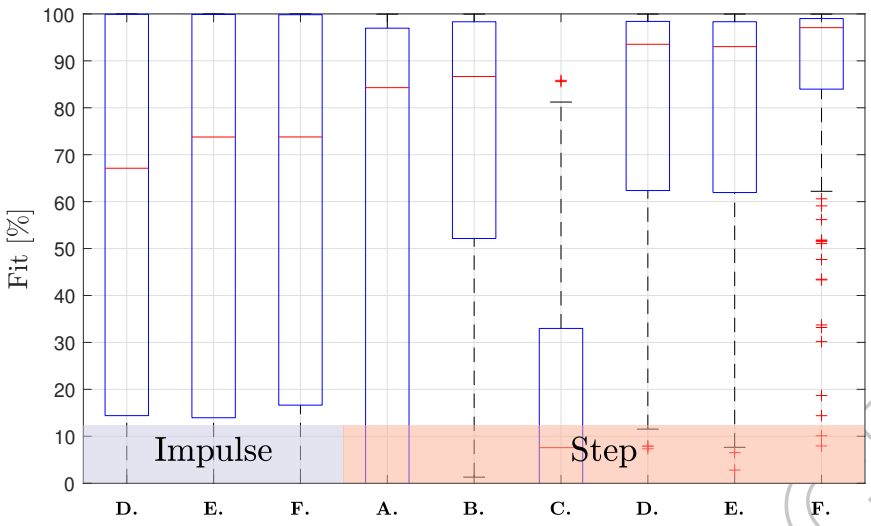


**Figure 5.** Performance of the considered methodologies on randomly selected systems. The plot shows the results using impulse response data (left) and step response data (right).

The term inside the integral can be simplified using the binomial theorem:

$$s_q(a,b) = \frac{1}{((q-1)!)^2} \int_0^a \sum_{i=0}^{q-1} \binom{q-1}{i} ((b-a)\,y)^{q-i-1} \left(y^2\right)^i dy$$
$$= \frac{1}{((q-1)!)^2} \sum_{i=0}^{q-1} \binom{q-1}{i} (b-a)^{q-i-1} \int_0^a y^{q+i-1}\, dy$$

Now, the integral can be solved and the expression can be rewritten as

$$s_q(a,b) = \frac{1}{((q-1)!)^2} \sum_{i=0}^{q-1} \binom{q-1}{i} \cdot \frac{(b-a)^{q-i-1}\, a^{q+i}}{q+i}$$

To further simplify this formulation, we can employ the binomial theorem a second time for the term

$$(b-a)^{q-i-1} = \sum_{j=0}^{q-i-1} \binom{q-i-1}{j} b^j\, (-a)^{q-i-1-j},$$

obtaining

$$s_q(a,b) = \sum_{i=0}^{q-1} \sum_{j=0}^{q-i-1} \alpha_q(i,j) \cdot a^{2q-j-1} \cdot b^j$$

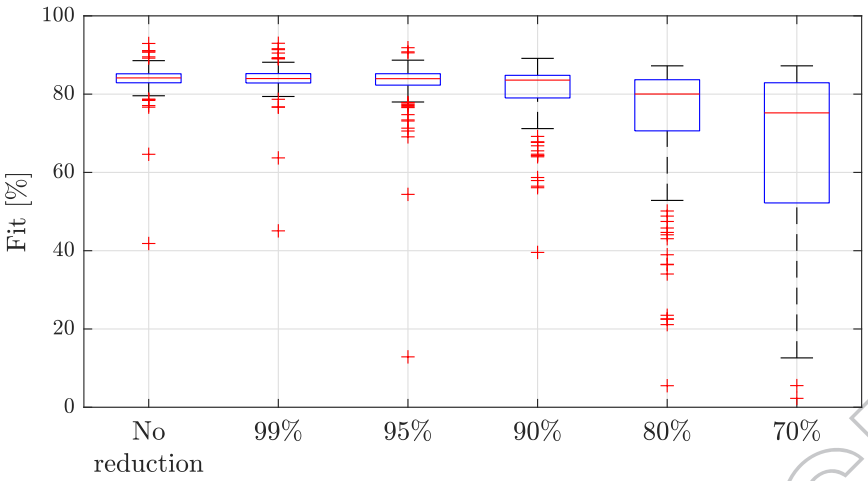


**Figure 6.** Performance on the test dataset using impulse response data for the system $G_2(s)$, for different levels of dimensionality reduction.

where

$$\alpha_q(i,j) = \binom{q-1}{i}\binom{q-i-1}{j}\frac{(-1)^{q-i-j-1}}{((q-1)!)^2(q+i)}$$

In order to remove one of the two summations, we note that

$$s_q(a,b) = \sum_{i=0}^{q-1}\sum_{j=0}^{q-1}\tilde{\alpha}_q(i,j)\cdot a^{2q-j-1}\cdot b^j$$

where

$$\tilde{\alpha}_q(i,j) = \begin{cases}\alpha_q(i,j) & \text{if } h \le q-i-1\\ 0 & \text{if } h > q-i-1\end{cases}$$

This is useful because, now, we can switch the summations order and bring all the terms that do not depend on $i$ upfront

$$s_q(a,b) = \sum_{j=0}^{q-1} a^{2q-j-1}\cdot b^j\cdot\left(\sum_{i=0}^{q-1}\tilde{\alpha}_q(i,j)\right) = \sum_{j=0}^{q-1}\gamma_{q,j}\cdot a^{2q-j-1}\cdot b^j$$

where

$$\gamma_{q,j} = \sum_{i=0}^{q-1}\tilde{\alpha}_q(i,j) = \sum_{j=0}^{q-i-1}\binom{q-1}{i}\binom{q-i-1}{j}\frac{(-1)^{q-i-j-1}}{((q-1)!)^2(q+i)}.$$

Using the binomial definition and some straightforward computations, it is possible to

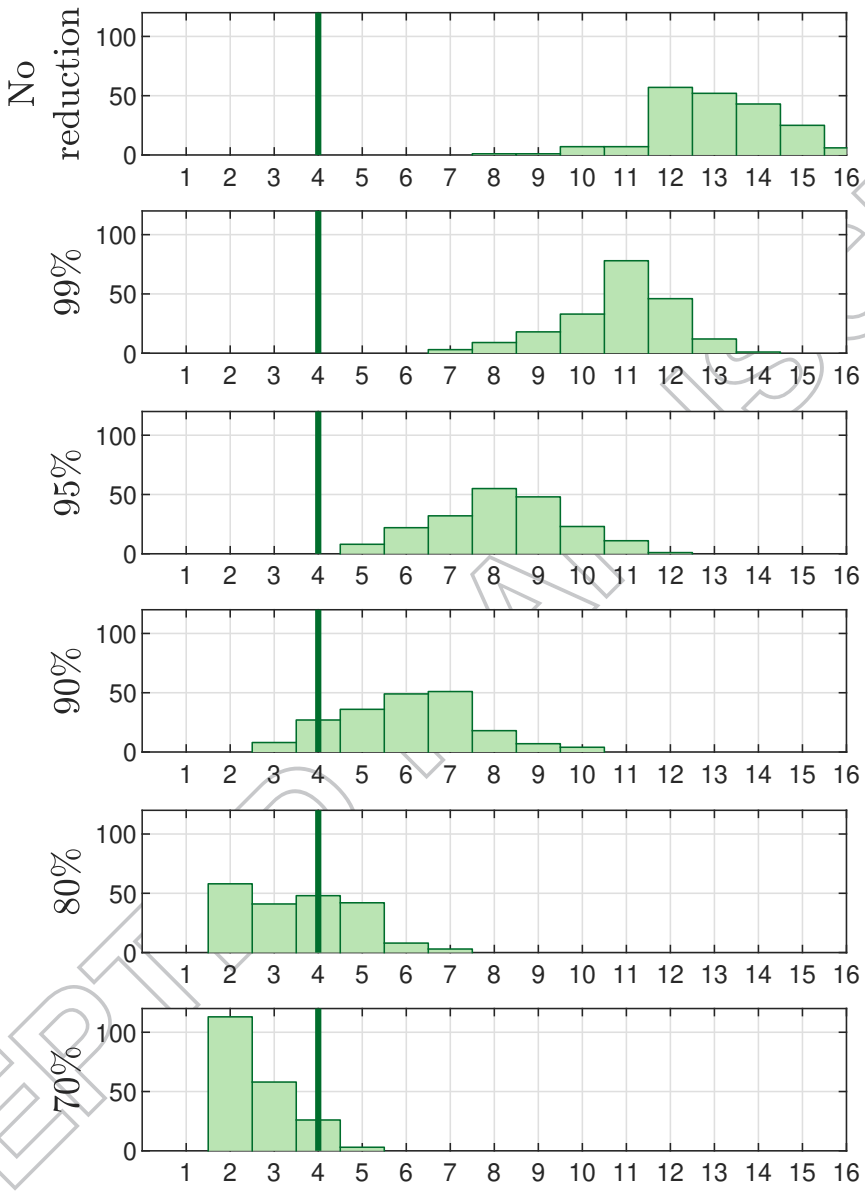


**Figure 7.** Histogram of the order of the estimated system at different level of dimensional reduction on the second benchmark model $G_2(s)$. The true system $G_2(s)$ has order 4, as indicated with the green vertical line.

rewrite $\gamma_{q,j}$ as

$$\gamma_{q,j} = \frac{(-1)^{q+j-1}}{j!\,(q-1)!} \cdot \sum_{i=0}^{q-j-1} \frac{(-1)^i}{i!\,(q-i-j-1)!\,(q+i)}$$

Now, thanks to the fact

$$\int_0^1 x^{q-1} \cdot (-x)^i \, dx = (-1)^i \cdot \left[\frac{x^{q+i}}{q+i}\right]_0^1 = \frac{(-1)^i}{q+i}$$

and defining

$$\beta_{q,j} = \frac{(-1)^{q+j-1}}{j!\,(q-1)!\,(q-j-1)!}.$$

we can note that

$$\begin{aligned}
\gamma_{q,j} &= \beta_{q,j} \cdot \sum_{i=0}^{q-j-1} \binom{q-j-1}{i} \int_0^1 x^{q-1} \cdot (-x)^i \, dx \\
&= \beta_{q,j} \cdot \int_0^1 x^{q-1} \underbrace{\sum_{i=0}^{q-j-1} \binom{q-j-1}{i} (-x)^i}_{(1-x)^{q-j-1}} \, dx \\
&= \beta_{q,j} \cdot \underbrace{\int_0^1 x^{q-1} \, (1-x)^{q-j-1} \, dx}_{B(q,q-j)} \\
&= \beta_{q,j} \cdot B\,(q, q-j)
\end{aligned}$$

where $B\,(a,b)$ is the Beta function (Olver, Lozier, Boisvert, & Clark, 2010). Recalling that

$$B\,(q, q-j) = \frac{(q-1)! \cdot (q-j-1)!}{(q+q-j-1)!}$$

It follows that

$$\gamma_{q,j} = \frac{(-1)^{q+j-1}}{j!\cancel{(q-1)!}\cancel{(q-j-1)!}} \cdot \frac{\cancel{(q-1)!}\cancel{(q-j-1)!}}{(2q-j-1)!} = \frac{(-1)^{q+j-1}}{j!\,(2q-j-1)!}$$

Let us, now, shift focus on the case where $a > b$. In this case, we can employ the fact that the kernel is a symmetric function to switch the two arguments and reusing

the same rationale as in the other case. In particular, we have

$$s_q(a,b) = s_q(b,a) = \sum_{j=0}^{q-1} \gamma_{q,j} \cdot b^{2q-j-1} \cdot a^j$$

Then,

$$s_q(a,b) = \sum_{h=0}^{q-1} \gamma_{q,h} \cdot \begin{cases} a^{2q-h-1} \cdot b^h & \text{if } a \leq b \\ b^{2q-h-1} \cdot a^h & \text{if } a > b \end{cases}$$

with

$$\gamma_{q,h} = \frac{(-1)^{q+h-1}}{h! \cdot (2q-h-1)!}$$

Concerning the second formula, from the definition of stable-spline, we have

$$k_q(a,b) = \lambda s_q\left(e^{-\beta a}, e^{-\beta b}\right)$$

Firstly, let us focus on the case where the first argument of the kernel is smaller than the second one, i.e. $a \geq b$. Here, using the results of Theorem 1 and by noting that $e^{-\beta a} \leq e^{-\beta b}$ because $\beta$ is strictly positive, we can write

$$\begin{aligned} k_q(a,b) &= \lambda \cdot \sum_{h=0}^{q-1} \gamma_{q,h} \cdot \left(e^{-\beta a}\right)^{2q-h-1} \cdot \left(e^{-\beta b}\right)^h \\ &= \lambda \cdot \sum_{h=0}^{q-1} \gamma_{q,h} \cdot e^{-\beta \cdot [(2q-h-1)\cdot a + h \cdot b]}. \end{aligned}$$

Analogously, in the case where $a < b$, we have

$$\begin{aligned} k_q(a,b) &= \lambda \cdot \sum_{h=0}^{q-1} \gamma_{q,h} \cdot \left(e^{-\beta b}\right)^{2q-h-1} \cdot \left(e^{-\beta a}\right)^h \\ &= \lambda \cdot \sum_{h=0}^{q-1} \gamma_{q,h} \cdot e^{-\beta \cdot [(2q-h-1)\cdot b + h \cdot a]} \end{aligned}$$

therefore:

$$k_q(a,b) = \lambda \sum_{h=0}^{q-1} \gamma_{q,h} \begin{cases} e^{-\beta \cdot [(2q-h-1)a + hb]} & \text{if } a \geq b \\ e^{-\beta \cdot [(2q-h-1)b + ha]} & \text{if } a < b \end{cases}$$

■

***Proof of Proposition 2.*** The transfer function of an LTI system corresponds to the Laplace transform of its impulse response. For this reason, we have

$$\hat{G}^u(s) = \mathcal{L}[\hat{g}^u](s) = \int_0^\infty \hat{g}^u(t)\, e^{-st}\, dt = \int_0^\infty \left( \sum_{i=1}^n c_i \hat{g}_i^u(t) \right) e^{-st}\, dt$$
$$= \sum_{i=1}^n c_i \int_0^\infty \hat{g}_i^u(t)\, e^{-st}\, dt = \sum_{i=1}^n c_i \hat{G}_i^u(s),$$

where the term $\hat{G}_i^u(s) = \mathcal{L}[\hat{g}_i^u](s)$ reads as

$$\hat{G}_i^u(s) = \int_0^\infty \hat{g}_i^u(t)\, e^{-st}\, dt = \int_0^\infty \left[ \int_0^\infty u(t_i - \xi)\, k(t, \xi)\, d\xi \right] e^{-st}\, dt$$
$$= \int_0^\infty u(t_i - \xi) \left[ \int_0^\infty k(t, \xi)\, e^{-st}\, dt \right] d\xi = \int_0^\infty u(t_i - \xi)\, K(s; \xi)\, d\xi.$$

To further simplify this expression, recall that the integral can be limited to $t_i - d$, obtaining

$$\hat{G}_i^u(s) = \int_0^{t_i - d} u(t_i - \xi)\, K(s; \xi)\, d\xi.$$

At last, with the change of variable $x = t_i - \xi$, we obtain

$$\hat{G}_i^u(s) = \int_d^{t_i} u(x)\, K(s; t_i - x)\, dx.$$

■

***Proof of Proposition 3.*** Let us start by analyzing the term

$$K_q(s; x) = \int_0^\infty k_q(x, t)\, e^{-st}\, dt,$$

where the kernel is a stable-spline of order $q$. It is useful to note that the parameter $x \in \mathbb{R}$ is always greater than 0 because in (19) this argument is always positive, thanks to the assumption that $t_i > d$.

It is convenient to divide this integral in two parts:

$$K_q(s; x) = \int_0^x k_q(x, t)\, e^{-st}\, dt + \int_x^\infty k_q(x, t)\, e^{-st}\, dt.$$

Firstly, let us focus on the first integral:

$$\begin{aligned}\int_0^x k_q(x,t)\,e^{-st}\,dt &= \int_0^x \lambda\sum_{h=0}^{q-1}\gamma_{q,h}e^{-\beta[(2q-h-1)x+ht]}e^{-st}\,dt\\ &= \lambda\sum_{h=0}^{q-1}\gamma_{q,h}e^{-\beta(2q-h-1)x}\int_0^x e^{-(s+\beta h)t}\,dt\\ &= \lambda\sum_{h=0}^{q-1}\gamma_{q,h}\frac{e^{-\beta(2q-h-1)x}}{s+\beta h}\left(1-e^{-(s+\beta h)x}\right)\\ &= \lambda\sum_{h=0}^{q-1}\gamma_{q,h}\left(\frac{e^{-\beta(2q-h-1)x}}{s+\beta h}-\frac{e^{-(s+\beta(2q-1))x}}{s+\beta h}\right).\end{aligned}$$

Analogously, the second integral can be simplified as

$$\begin{aligned}\int_x^\infty k_q(x,t)\,e^{-st}\,dt &= \int_x^\infty \lambda\sum_{h=0}^{q-1}\gamma_{q,h}e^{-\beta[(2q-h-1)t+hx]}e^{-st}\,dt\\ &= \lambda\sum_{h=0}^{q-1}\gamma_{q,h}e^{-\beta hx}\int_x^\infty e^{-(s+\beta(2q-h-1))t}\,dt\\ &= \lambda\sum_{h=0}^{q-1}\gamma_{q,h}\frac{e^{-(s+\beta(2q-h-1))x}}{s+\beta(2q-h-1)}.\end{aligned}$$

Thus, $K_q(s;x)$ can be reformulated as

$$K_q(s;x)=\lambda\sum_{h=0}^{q-1}\gamma_{q,h}\frac{e^{-\beta(2q-h-1)x}}{s+\beta h}+\lambda\sum_{h=0}^{q-1}\gamma_{q,h}\left[\frac{e^{-(s+\beta(2q-1))x}}{s+\beta(2q-h-1)}-\frac{e^{-(s+\beta(2q-1))x}}{s+\beta h}\right].$$

This can be further simplified by noting that

$$\sum_{h=0}^{q-1}\gamma_{q,h}\left(\frac{1}{s+\beta(2q-h-1)}-\frac{1}{s+\beta h}\right)=\frac{(-1)^q\,\beta^{2q-1}}{\prod_{i=0}^{2q-1}(s+\beta i)},$$

obtaining

$$K_q(s;x)=\lambda\sum_{h=0}^{q-1}\gamma_{q,h}\frac{e^{-\beta(2q-h-1)x}}{s+\beta h}+\lambda e^{-(s+\beta(2q-1))x}\frac{(-1)^q\,\beta^{2q-1}}{\prod_{i=0}^{2q-1}(\beta i+s)}.$$

Now, it is possible to plug $K_q(s;x)$ in (19) to obtain $\hat{G}_i^u$ for the stable-spline kernel.

$$\begin{aligned}
G_i^u(s) &= \int_d^{t_i} u(\tau)\, K(s; t_i - \tau)\, d\tau \\
&= \lambda \sum_{h=0}^{q-1} \frac{\gamma_{q,h}}{s+\beta h} \underbrace{\int_d^{t_i} u(\tau)\, e^{-\beta(2q-h-1)(t_i-\tau)}\, d\tau}_{B_i^u(\beta(2q-h-1))} + \\
&\quad + \lambda \frac{(-1)^q\, \beta^{2q-1}}{\prod_{i=0}^{2q-1}(\beta i + s)} \underbrace{\int_d^{t_i} u(\tau)\, e^{-(s+\beta(2q-1))(t_i-\tau)}\, d\tau}_{B_i^u(s+\beta(2q-1))} \\
&= \lambda \sum_{h=0}^{q-1} \frac{\gamma_{q,h}}{s+\beta h} B_i^u(\beta(2q-h-1)) + \lambda \frac{(-1)^q\, \beta^{2q-1}}{\prod_{i=0}^{2q-1}(\beta i + s)} B_i^u(s+\beta(2q-1)).
\end{aligned}$$

Where

$$B_i^u(x) = \int_d^{t_i} u(\tau)\, e^{-x(t_i-\tau)}\, d\tau$$

with a change of variable, we can note that

$$B_i^u(x) = -\int_{t_i-d}^{d} u(t_i-\xi)\, e^{-x\xi}\, d\xi = \int_0^{t_i-d} u(t_i-\xi)\, e^{-x\xi}\, d\xi$$

since $u(t) = 0$, $\forall t \le d$, we can extend the integral upper bound to infinity.

$$B_i^u(x) = \int_0^{\infty} u(t_i-\xi)\, e^{-x\xi}\, d\xi = \mathcal{L}[u_i](x) = A_i^u(x)$$

Lastly, the identified transfer function using the stable-spline kernel is then

$$\begin{aligned}\hat{G}^u(s) &= \sum_{i=1}^{n} c_i \hat{G}_i^u(s) \\ &= \lambda \sum_{h=0}^{q-1} \underbrace{\frac{\gamma_{q,h}}{s+\beta h} \sum_{i=1}^{n} c_i A_i^u(\beta(2q-h-1))}_{Q_{q,h}^u(s)} + \\ &\quad + \lambda \underbrace{\frac{(-1)^q \beta^{2q-1}}{\prod_{i=0}^{2q-1}(s+\beta i)} \sum_{i=1}^{n} c_i A_i^u(s+\beta(2q-1))}_{H_q^u(s)} \\ &= \lambda \left[ \sum_{h=0}^{q-1} Q_{q,h}^u(s) + H_q^u(s) \right].\end{aligned}$$

■

***Proof of Theorem 1.*** Since the transfer function $\hat{G}^u$ is defined as the sum of $q+1$ transfer functions, we need to show that all these addends are asymptotically stable. First, let us consider the $q-1$ addends of the type

$$Q_{q,h}^u(s) = \lambda \cdot \frac{\gamma_{q,h}}{s+\beta h} \cdot \left( \sum_{i=1}^{n} c_i A_i^u(\beta(2q-h-1)) \right),$$

with $h > 0$. All these rational functions have only one real pole in $-\beta h$ and it is strictly less than zero because $h > 0$ and $\beta > 0$. Therefore, these first $q-1$ transfer functions are asymptotically stable. The remainder of $\hat{G}^u$ is

$$\begin{aligned}R(s) &= \lambda Q_{q,0}^u(s) + \lambda H_q^u(s) \\ &= \frac{\lambda}{s} \cdot \gamma_{q,0} \sum_{i=1}^{n} c_i A_i^u(\beta(2q-1)) + \frac{\lambda}{s} \cdot \frac{(-1)^q \beta^{2q-1}}{\prod_{i=1}^{2q-1}(\beta i + s)} \sum_{i=1}^{n} c_i A_i^u(s+\beta(2q-1)).\end{aligned}$$

The poles of the transfer function $R(s)$ are

$$\{0, -\beta, -2\beta, \ldots, -(2q-1)\beta\} \cup \left( \bigcup_{i=1}^{n} \mathcal{P}_i \right),$$

where $\mathcal{P}_i$ are the poles, whose real part is strictly negative (for the hypothesis of the Theorem), of the transfer function $A_i^u(s+\beta(2q-1))$. Therefore, the only non-strictly negative pole is the one in 0 because $\beta > 0$. However, there is also a zero in the origin. To see this, consider the transfer function $\widetilde{R}(s)$ such that $R(s) = \frac{\lambda}{s} \cdot \tilde{R}(s)$. Then, the transfer function $R(s)$ has a zero in the origin if and only if $R(0) = 0$. This can be

verified with some mathematical steps

$$\begin{aligned}\tilde{R}(0) &= \gamma_{q,0}\sum_{i=1}^{n} c_i A_i^u\left(\beta\left(2q-1\right)\right) + \frac{(-1)^q\,\beta^{2q-1}}{\prod_{i=1}^{2q-1}\beta i}\sum_{i=1}^{n} c_i A_i^u\left(\beta\left(2q-1\right)\right)\\ &= \left(\frac{(-1)^{q-1}}{(2q-1)!} + \frac{(-1)^q\,\cancel{\beta^{2q-1}}}{\cancel{\beta^{2q-1}}\,(2q-1)!}\right)\sum_{i=1}^{n} c_i A_i^u\left(\beta\left(2q-1\right)\right)\\ &= \frac{(-1)^{q-1}+(-1)^q}{(2q-1)!}\sum_{i=1}^{n} c_i A_i^u\left(\beta\left(2q-1\right)\right).\end{aligned}$$

Since $(-1)^{q-1}$ and $(-1)^q$ have opposite signs for every value of $q$, we have

$$\tilde{R}(0) = \frac{0}{(2q-1)!}\sum_{i=1}^{n} c_i A_i^u\left(\beta\left(2q-1\right)\right) = 0$$

therefore $R(s)$ has a zero in the origin that cancels out the pole in 0. Therefore, the identified system $\hat{G}^u$ is asymptotically stable.

■

## References


Aravkin, A. Y., Burke, J. V., & Pillonetto, G. (2018, January). Generalized system identification with stable spline kernels. *SIAM Journal on Scientific Computing*, *40*(5), B1419–B1443.

Baker, G. A., & Graves-Morris, P. (1996). *Padé approximants* (Vol. 59). Cambridge University Press.

Bottegal, G., Risuleo, R. S., & Hjalmarsson, H. (2015). Blind system identification using kernel-based method. *IFAC-PapersOnLine*, *48*(28), 466–471. (17th IFAC Symposium on System Identification SYSID 2015)

Chen, F., Agüero, J. C., Gilson, M., Garnier, H., & Liu, T. (2017, March). Em-based identification of continuous-time arma models from irregularly sampled data. *Automatica*, *77*, 293–301.

Chen, F., Garnier, H., & Gilson, M. (2015, January). Robust identification of continuous-time models with arbitrary time-delay from irregularly sampled data. *Journal of Process Control*, *25*, 19–27.

Chen, T. (2018a, December). Continuous-time DC kernel—a stable generalized first-order spline kernel. *IEEE Transactions on Automatic Control*, *63*(12), 4442–4447.

Chen, T. (2018b, April). On kernel design for regularized LTI system identification. *Automatica*, *90*, 109–122.

Chen, T., Ardeshiri, T., Carli, F. P., Chiuso, A., Ljung, L., & Pillonetto, G. (2016, April). Maximum entropy properties of discrete-time first-order stable spline kernel. *Automatica*, *66*, 34–38.

Chen, T., Ohlsson, H., & Ljung, L. (2012, August). On the estimation of transfer functions, regularizations and gaussian processes—revisited. *Automatica*, *48*(8), 1525–1535.

Darwish, M. A. H., Cox, P. B., Proimadis, I., Pillonetto, G., & Tóth, R. (2018, November). Prediction-error identification of LPV systems: A nonparametric gaussian regression approach. *Automatica*, *97*, 92–103.

Dinuzzo, F. (2015). Kernels for linear time invariant system identification. *SIAM Journal on Control and Optimization*, *53*(5), 3299–3317.

Dinuzzo, F., & Schölkopf, B. (2012). The representer theorem for hilbert spaces: a necessary and sufficient condition. In F. Pereira, C. J. C. Burges, L. Bottou, & K. Q. Weinberger (Eds.), *Advances in neural information processing systems 25* (pp. 189–196). Curran Associates, Inc.

Formentin, S., Mazzoleni, M., Scandella, M., & Previdi, F. (2019, June). Nonlinear system identification via data augmentation. *Systems & Control Letters*, *128*, 56–63.

Garnier, H. (2015, July). Direct continuous-time approaches to system identification. overview and benefits for practical applications. *European Journal of Control*, *24*, 50–62. (SI: ECC15)

Garnier, H., & Gilson, M. (2018). CONTSID: a matlab toolbox for standard and advanced identification of black-box continuous-time models. *IFAC-PapersOnLine*, *51*(15), 688–693. (18th IFAC Symposium on System Identification SYSID 2018)

Garnier, H., & Wang, L. (2008). *Identification of continuous-time models from sampled data*. Springer London.

Garnier, H., & Young, P. C. (2012, July). What does continuous-time model identification have to offer? *IFAC Proceedings Volumes*, *45*(16), 810–815. (16th IFAC Symposium on System Identification)

Golabi, A., Meskin, N., Toth, R., & Mohammadpour, J. (2017, November). A bayesian approach for LPV model identification and its application to complex processes. *IEEE Transactions on Control Systems Technology*, *25*(6), 2160–2167.

Lataire, J., Pintelon, R., Piga, D., & Tóth, R. (2017, February). Continuous-time linear time-varying system identification with a frequency-domain kernel-based estimator. *IET Control Theory & Applications*, *11*(4), 457–465.

Ljung, L., & Glad, T. (2016). *Modeling & identification of dynamic systems*. Studentlitteratur AB.

Mazzoleni, M., Formentin, S., Scandella, M., & Previdi, F. (2018, June). Semi-supervised learning of dynamical systems: a preliminary study. In *2018 european control conference (ecc)* (pp. 2824–2829). IEEE.

Mazzoleni, M., Scandella, M., Formentin, S., & Previdi, F. (2018, December). Classification of light charged particles via learning-based system identification. In *2018 IEEE conference on decision and control (CDC)* (pp. 6053–6058). IEEE.

Mazzoleni, M., Scandella, M., & Previdi, F. (2019). A comparison of manifold regularization approaches for kernel-based system identification. *Accepted for publication in Proceedings of the 13th IFAC Workshop on Adaptive and Learning Control Systems (ALCOS-2019), Guildhall Winchester, Winchester, United Kingdom*.

Olver, F. W. J., Lozier, D. W., Boisvert, R. F., & Clark, C. W. (2010). *Nist handbook of mathematical functions hardback and cd-rom* (C. university press, Ed.). Cambridge University Press.

Padilla, A., Garnier, H., Young, P. C., Chen, F., & Yuz, J. I. (2019, December). Identification of continuous-time models with slowly time-varying parameters. *Control Engineering Practice*, *93*, 104165.

Paduart, J., Lauwers, L., Swevers, J., Smolders, K., Schoukens, J., & Pintelon, R. (2010, April). Identification of nonlinear systems using polynomial nonlinear state space models. *Automatica*, *46*(4), 647–656.

Pascu, V., Garnier, H., Ljung, L., & Janot, A. (2019, September). Benchmark problems for continuous-time model identification: Design aspects, results and perspectives. *Automatica*, *107*, 511–517.

Pillonetto, G. (2015, September). Identification of hybrid systems using stable spline kernels. In *2015 ieee 25th international workshop on machine learning for signal processing (mlsp)* (pp. 1–6).

Pillonetto, G. (2018, July). System identification using kernel-based regularization: New insights on stability and consistency issues. *Automatica*, *93*, 321–332.

Pillonetto, G., Carè, A., & Campi, M. C. (2018). Kernel-based SPS. *IFAC-PapersOnLine*, *51*(15), 31–36. (18th IFAC Symposium on System Identification SYSID 2018)

Pillonetto, G., Chiuso, A., & De Nicolao, G. (2019, October). Stable spline identification of linear systems under missing data. *Automatica*, *108*, 108493.

Pillonetto, G., & De Nicolao, G. (2010, January). A new kernel-based approach for linear system identification. *Automatica*, *46*(1), 81–93.

Pillonetto, G., Dinuzzo, F., Chen, T., De Nicolao, G., & Ljung, L. (2014, March). Kernel methods in system identification, machine learning and function estimation: A survey. *Automatica*, *50*(3), 657–682.

Pillonetto, G., Quang, M. H., & Chiuso, A. (2011, December). A new kernel-based approach for NonlinearSystem identification. *IEEE Transactions on Automatic Control*, *56*(12), 2825–2840.

Pintelon, R., Guillaume, P., Rolain, Y., Schoukens, J., & Hamme, H. V. (1994, November). Parametric identification of transfer functions in the frequency domain-a survey. *IEEE Transactions on Automatic Control*, *39*(11), 2245–2260.

Pintelon, R., & Schoukens, J. (2012). *System identification*. John Wiley & Sons.

Rao, G. P., & Garnier, H. (2002). Numerical illustrations of the relevance of direct continuous-time model indentification. *IFAC Proceedings Volumes*, *35*(1), 133–138. (15th IFAC World Congress)

Risuleo, R. S., Bottegal, G., & Hjalmarsson, H. (2015, December). A new kernel-based approach to overparameterized Hammerstein system identification. In *2015 54th ieee conference on decision and control (cdc)* (pp. 115–120).

Rudi, A., Camoriano, R., & Rosasco, L. (2015). Less is more: Nyström computational regularization. In C. Cortes, N. D. Lawrence, D. D. Lee, M. Sugiyama, & R. Garnett (Eds.), *Advances in neural information processing systems 28* (pp. 1657–1665). Curran Associates, Inc.

Rudi, A., Carratino, L., & Rosasco, L. (2017). Falkon: An optimal large scale kernel method. In I. Guyon et al. (Eds.), *Advances in neural information processing systems* (pp. 3888–3898). Curran Associates, Inc.

Rüdinger, F., & Krenk, S. (2001, July). Non-parametric system identification from non-linear stochastic response. *Probabilistic Engineering Mechanics*, *16*(3), 233–243.

Scandella, M., Mazzoleni, M., Formentin, S., & Previdi, F. (2020). A note on the numerical solutions of kernel-based learning problems. *IEEE Transactions on Automatic Control*, 1–1.

Schoukens, J., Pintelon, R., Vandersteen, G., & Guillaume, P. (1997, June). Frequency-domain system identification using non-parametric noise models estimated from a small number of data sets. *Automatica*, *33*(6), 1073–1086.

Shi, Z. Y., Law, S. S., & Xu, X. (2009, April). Identification of linear time-varying mdof dynamic systems from forced excitation using hilbert transform and EMD method. *Journal of Sound and Vibration*, *321*(3), 572–589.

Varga, A. (1991, December). Balancing free square-root algorithm for computing singular perturbation approximations. In *Proceedings of the 30th ieee conference on decision and control* (Vol. 2, pp. 1062–1065). IEEE.

Velleman, P. F., & Hoaglin, D. C. (1981). *Applications, basics, and computing of exploratory data analysis*. Duxbury Press.

Wahba, G. (1990). *Spline models for observational data*. SIAM: Society for Industrial and Applied Mathematics.

Wang, L., & Gawthrop, P. (2001, January). On the estimation of continuous time transfer functions. *International Journal of Control*, *74*(9), 889–904.

Wellstead, P. E. (1981, January). Non-parametric methods of system identification. *Automatica*, *17*(1), 55–69.

Young, P. C. (2011). *Recursive estimation and time-series analysis*. Springer Berlin Heidelberg.

Young, P. C. (2015, February). Refined instrumental variable estimation: Maximum likelihood optimization of a unified box–jenkins model. *Automatica*, *52*, 35–46.